Available online at www.sciencedirect.com

SciVerse ScienceDirect

journal homepage: www.elsevier.com/locate/acme

Original Research Article

Non-destructive investigation of corrosion current density in steel reinforced concrete by artificial neural networks

L. Sadowski

Wroclaw University of Technology, Institute of Building Engineering, Wybrzeze Wyspianskiego 27, 50-370 Wroclaw, Poland

ARTICLE INFO

Article history:
Received 30 July 2012
Accepted 28 October 2012
Available online 3 November 2012

Keywords:
Steel reinforced concrete
Non-destructive testing
Artificial intelligence
Resistivity
Polarisation

ABSTRACT

Corrosion of the steel reinforcement in concrete is an important problem for the civil engineering. Inspection techniques are needed to assess the corrosion in order to protect and repair concrete structures. Many studies were performed to establish a series of corrosion rate assessment methods. A method of providing a direct evaluation of the corrosion rate by corrosion current density measurement is Linear Polarisation Resistance (LPR). The main drawback is that it requires a localised breakout of the concrete cover. The corrosion of the steel reinforcement is monitored by measuring the resistivity of the concrete. The purpose of this paper is to use the resistivity four-probe method and galvanostatic resistivity measurement together with neural networks to assess the corrosion rate of steel in concrete without a direct connection to the reinforcement. Three parameters determined by two non-destructive resistivity methods together with the air temperature were employed as input variables, and corrosion current density, predicted by the destructive LPR method, acted as the output variable. The results shows that it is possible to predict corrosion current density in steel reinforced concrete by using the model based on artificial neural networks on the basis of parameters determined by two non-destructive resistivity measurement techniques.

1. Introduction

Steel reinforced concrete is one of the most durable construction materials, but corrosion is the main cause of deterioration of reinforced concrete structures. Steel reinforcement corrosion is initiated and propagates unseen beneath the concrete cover, and it is difficult to evaluate the severity of the problem [1,2]. In the existing literature, many studies were performed to establish a series of models on the corrosion of steel in concrete, such as numerical simulations or general linear models [3–5].

In recent decades one of the most promising methods of providing a direct evaluation of the corrosion rate by corrosion current density i_{corr} measurement has been Linear Polarisation Resistance (LPR), which is known to be a method having certain limitations. LPR has its drawbacks in terms of accurate estimates of corrosion current densities when chloride contamination is present and pitting corrosion is taking place. Also, one of the main drawbacks of this destructive technique is that in order to provide an electrical connection to the steel reinforcement, it requires a localised breakout of the concrete cover [6–9].

E-mail address: lukasz.sadowski@pwr.wroc.pl

1644-9665/$ - see front matter © 2012 Politechnika Wrocławska. Published by Elsevier Urban & Partner Sp. z o.o. All rights reserved.
http://dx.doi.org/10.1016/j.acme.2012.10.007

In many cases, the corrosion of the steel reinforcement is monitored by measuring the resistivity of the concrete. The concrete four-probe resistivity measurement method used in the following article was adapted from a technique initially used for geophysical surveying [10]. In this technique, a low magnitude alternating current (AC) is passed through the concrete using two surface electrodes. It can be inferred from the measurement of low resistivity that if steel reinforcement corrosion is in progress then the rate of corrosion will be high. In this method it is possible to measure concrete resistivity over the steel bar $\rho_{AC,bar}$ as well as concrete resistivity $\rho_{AC,conc}$. It should also be noted that there are existing published correlations in the literature between corrosion probability and resistivity, and between chloride diffusion and resistivity in concrete [11–15]. It is proper to note that the measurement of concrete resistivity provides additional information to assist in assessing corrosion activity, and is a useful supplement to a half-cell potential survey. The main limitation of this method is that it indicates the probability of corrosion location and activity, but it does not provide a direct measurement of the steel reinforcement corrosion rate.

Researchers have established many modifications to conventional four-probe resistivity measurement [16,17]. One of these versions is galvanostatic resistivity measurement [18]. This technique takes advantage of the short-circuit effect of a steel bar on the resistivity method, and the resistivity measurements are taken using a modified electrode array. The two inner standard resistivity probes are replaced with two copper–copper sulphate reference electrodes, and the outer resistivity probes are adopted from the conventional resistivity measurement. The purpose of this method is to measure DC resistivity ρ_{DC}.

It is also well known that the concrete degradation and corrosion of steel reinforcement depends on environmental conditions, on concrete properties or on moisture content [19–21]. These parameters have an influence on measured concrete resistivity for both the conventional four-probe resistivity measurement and for galvanostatic resistivity measurement. Considering the above, it seems sensible to employ more parameters in one model to obtain a more accurate answer concerning the corrosion of steel reinforcement than that given by correlations between single parameters. The aim of the tests was to find whether artificial neural networks could be used for this purpose.

Artificial neural networks (ANN) are computational structures whose architecture has been inspired from our knowledge about biological neural networks in the human nervous system [22]. ANN analysis is a functional tool for investigating and predicting the performance of scenarios with varying situations and systems that cannot be described by any analytical equations. Over the last few years, neural networks have emerged as a powerful device that could be used in many civil engineering applications [23–27].

Researchers have developed a series of models on the corrosion of steel using neural networks and support vector regression [28–30]. The application of ANN for predicting corrosion current density is limited in the literature [31]. No study has been carried out to predict corrosion current density based on parameters determined by the concrete resistivity four-probe method and the galvanostatic resistivity measurement together with the neural network approach.

The objective of this work is to use the resistivity four-probe method and galvanostatic resistivity measurement together with neural networks to assess the corrosion rate of steel in concrete without a direct connection to the reinforcement. The most popular ANN for this purpose is the multilayer perceptron neural network (MLP-NN). The MLP-NN has an input layer, one or more hidden layers and an output layer. Computations take place in the hidden and output layers. Theoretical works have shown that a single hidden layer is sufficient for an ANN [32–35]. Therefore, in this study, one hidden layer is used.

2. Materials and methods

This section describes the experimental details and database used in this paper and presents the methodology that was applied.

2.1. *Experimental details and database*

To use ANN for corrosion current density prediction, a database is needed for the training and testing of MLP-NN.

Specimens sized 400 mm × 300 mm × 100 mm were available, with each specimen containing a single, short steel bar 30 mm in diameter, made from steel class A-III grade 34GS. The slabs were made from concrete class C 20/25 and from Portland cement CEM I 42.5R and aggregate of maximum size—5 mm. Since the relative humidity of concrete has a significant influence on the concrete resistivity, the specimens were stored in a laboratory under constant relative concrete humidity conditions of 65% ± 1% up to the time of the tests. A view of the laboratory stand is presented in Fig. 1 [18]. The study was carried out based on a database of concrete slabs of two different conditions. Slabs *A* and *B* had high and moderate corrosion rates, respectively, with laboratory-induced corrosion as presented previously [18].

In the following article the exemplary steel corrosion data, measured by using the resistivity method, galvanostatic resistivity measurement and the LPR method, were listed in Tables 1 and 2. The database presented in Table 1 includes

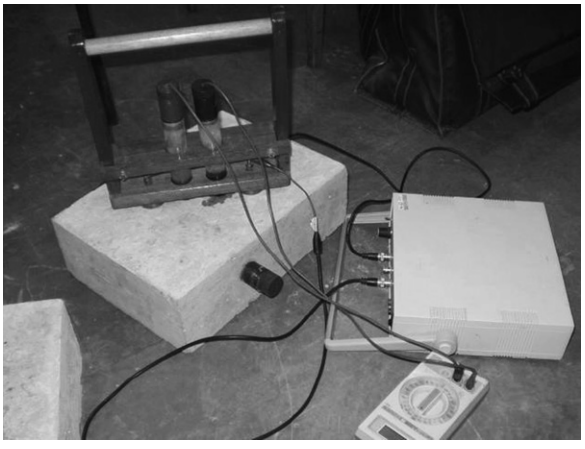

Fig. 1 – Laboratory stand [18].

Table 1 – Exemplary steel corrosion data for slab A.

No.	T (°C)	$\rho_{AC,bar}$ (kΩ cm)	$\rho_{AC,coc}$ (kΩ cm)	ρ_{DC} (kΩ cm)	i_{corr} (μA/cm^2)
1	21.00	3.15	24.93	3.75	8.412
2	20.80	3.16	24.99	3.81	8.425
3	20.50	3.18	25.12	3.86	8.436
4	20.10	3.19	25.28	3.88	8.441
5	19.80	3.20	25.59	3.89	8.452
6	19.50	3.21	25.62	3.92	8.464
7	19.20	3.22	25.65	3.94	8.471
8	19.00	3.23	23.27	4.01	8.489
9	20.90	3.03	23.35	3.57	8.344
10	20.70	3.05	23.42	3.59	8.361
.	.	.	.	.	.
.	.	.	.	.	.
.	.	.	.	.	.
16	19.30	3.13	23.86	3.71	8.480
.	.	.	.	.	.
.	.	.	.	.	.
.	.	.	.	.	.
50	19.30	3.12	23.87	3.72	8.477
.	.	.	.	.	.
.	.	.	.	.	.
.	.	.	.	.	.
68	19.10	3.16	23.92	2.76	8.411

Table 2 – Exemplary steel corrosion data for slab B.

No.	T (°C)	$\rho_{AC,bar}$ (kΩ cm)	$\rho_{AC,coc}$ (kΩ cm)	ρ_{DC} (kΩ cm)	i_{corr} (μA/cm^2)
1	21.00	19.31	22.27	21.81	0.422
2	20.80	19.33	22.28	21.83	0.423
3	20.50	19.34	22.30	21.85	0.421
4	20.10	19.35	22.31	21.91	0.439
5	19.80	19.36	22.32	21.92	0.439
6	19.50	19.36	22.33	21.94	0.456
7	19.20	19.37	22.36	21.96	0.466
8	19.00	19.38	22.38	21.98	0.476
9	20.90	19.24	22.09	21.62	0.373
10	20.70	19.25	22.12	21.63	0.380
.	.	.	.	.	.
.	.	.	.	.	.
.	.	.	.	.	.
48	19.70	19.28	22.19	21.69	0.487
.	.	.	.	.	.
.	.	.	.	.	.
.	.	.	.	.	.
68	19.10	19.30	22.22	21.77	0.421

exemplary data for concrete slab A. Conversely, the database presented in Table 2 includes exemplary data for concrete slab B. The parameters considered in the study are: air temperature (T), AC resistivity over the steel bar ($\rho_{AC,bar}$), AC resistivity remote from the steel bar ($\rho_{AC,conc}$), DC resistivity over the steel bar (ρ_{DC}), and corrosion current density (i_{corr}).

2.2. *Methodology*

The methodology for predicting the corrosion current density of steel in concrete with the use of ANN is schematically described in Fig. 2. Three stages can be distinguished in the scheme.

The experimental results forming a set of data and used for the training and testing of the MLP-NN are an integral part of stage 1, in which four parameters were employed as input variables:

a) air temperature (*T*),
b) AC resistivity over the steel bar ($\rho_{AC,bar}$),
c) AC resistivity remote from the steel bar ($\rho_{AC,conc}$),
d) DC resistivity over the steel bar (ρ_{DC}).

Corrosion current density (i_{corr}) acted as an output variable.

In stage 2 the experimental results were used as input data for the training and testing of the MLP-NN. Before applying the MLP-NN to the data, the input and output values were normalised using the following equation [22]:

$$a\frac{y_i - y_{min}}{y_{max} - y_{min}} + b \quad (1)$$

where y_{min} and y_{max} denote the minimum and maximum of the input and output data, and y_i represents the ith target value. The values of the scaling factors, a and b, were taken as 0.6 and 0.2 [36]. The MLP-NN models were learnt by using training samples, the parameters (T, $\rho_{AC,bar}$, $\rho_{AC,conc}$, ρ_{DC}) were optimised through continuous training adjustment. The results were evaluated using two indexes, i.e. correlation coefficients (R^2) and mean percentage error (*MAPE*). The indexes are formulated by equations [37,38]:

$$R^2 = \frac{\sum_{i=1}^{n}\left(\hat{d}_i - \bar{y}\right)^2}{\sum_{i=1}^{n}\left(d_i - \bar{y}\right)^2} \quad (2)$$

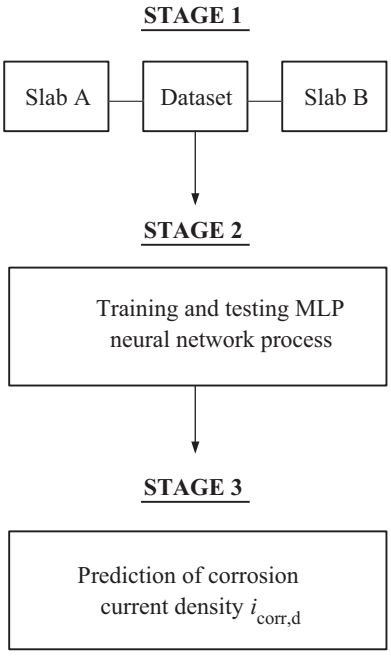

Fig. 2 – Block diagram of current density identification by means of neural networks on the basis of non-destructive resistivity measurements.

$$MAPE = \frac{1}{n}\sum_{i=1}^{n}\left|\frac{d_i - y_i}{y_i}\right| \quad (3)$$

where n denotes the number of test samples, y_i represents the ith target value, d_i stands for the predicted value for the ith test sample and $\bar{y}$ is the mean target value for all test samples. Then, MLP-NN with one hidden layer was trained and optimised for predicting the behaviour of the system under investigation. The training process is used to adjust the network weights and to determine when to terminate the training. The back propagation (BP) training algorithm was used here to adjust the weights. This training algorithm was selected because of its proven mapping capabilities and widespread application in civil engineering, and 15% of the total data were divided for testing [39–42]. Finally, at the end of stage 2 the input data were denormalised.

The obtained results were investigated in stage 3, whose output was predicted as corrosion current density $i_{corr,d}$.

3. Results and discussion

The investigation and prediction of corrosion current density was carried out with two sets of training and testing data. The results of the investigations for slab *A* and slab *B*, together with the MLP-NN verification stage and the corresponding predictions, are discussed below.

3.1. *Slab A*

From this set the data were divided into data for training (70% of the total data) and testing (15% of the total data). The data from the training set were used to determine the number of neurons in the hidden layer. After the end of the testing process, the remaining 15% among all the data sets were randomly selected for MLP-NN verification.

The number of neurons evaluated ranged from 3 to 9. As can be seen in Table 3, the *MAPE* error is minimal when the number of neurons in the hidden layer is 5. Table 3 also lists the correlation coefficients R^2 of MLP networks, and their correlation coefficients are also the highest when the number of neurons in the hidden layer is 5.

The architecture of MLP-NN obtained for this test is illustrated in Fig. 3. The network was generalised with an input layer, one hidden layer with 5 neurons in number and an output layer.

Table 3 – Evaluation on the prediction results (slab *A*).

No.	MLP-NN architecture	R^2 (–)		*MAPE* (–)	
		Training	Testing	Training	Testing
1	4-3-1	0.942733	0.982663	0.000091	0.000036
2	4-4-1	0.940467	0.971460	0.000095	0.000049
3	**4-5-1**	**0.943629**	**0.984322**	**0.000090**	**0.000035**
4	4-6-1	0.941018	0.975823	0.000094	0.000042
5	4-7-1	0.939110	0.977184	0.000097	0.000040
6	4-8-1	0.934855	0.976623	0.000098	0.000038
7	4-9-1	0.943459	0.983469	0.000090	0.000026

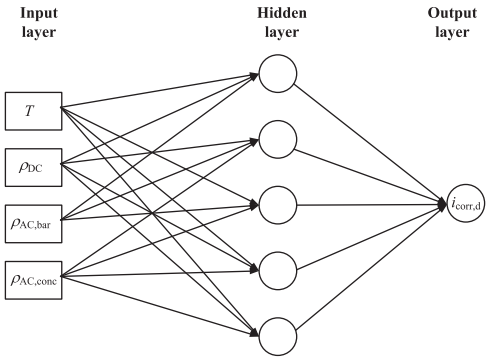

Fig. 3 – The architecture of MLP-NN obtained for slab A.

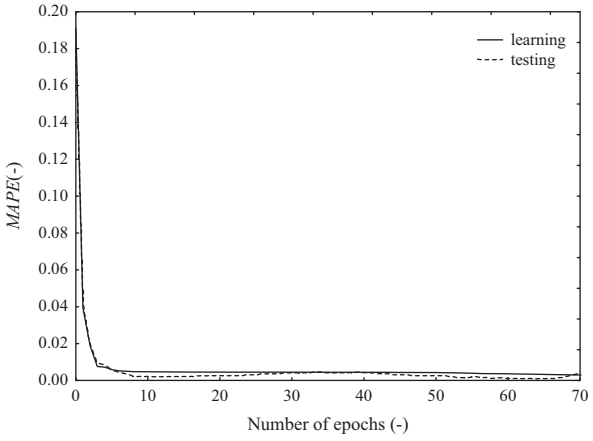

Fig. 4 – MLP-NN training and testing MAPE versus the number of epochs (slab A).

It is evident that the MAPE error in the training and testing process decreases rapidly with the growing number of epochs, and stabilises at a level of about 0.000090. It is presented in Fig. 4.

The predicted values of corrosion current density $i_{corr,d}$ in the training process (MLP-NN output when the test data set is used as input into the network) for different times of measurement plotted against the experimentally measured values of corrosion current density i_{corr}, are shown in Fig. 5. The correlation coefficient R^2 was observed to be 0.943629, indicating that the fit has a high degree of precision. However, it is obvious that the two points, with an estimated value of 8.423 μA/cm^2 and 8.431 μA/cm^2 in Fig. 6, are a deviation from the straight line. These points came from the test samples numbered as 50 and 16; the target value (8.477 μA/cm^2 and 8.480 μA/cm^2) was the largest among all of the training values, although the MAPE error in the training process was observed to be 0.000090.

In the testing process the predicted values of corrosion current density $i_{corr,d}$ for different times of measurement were plotted against the experimentally measured values of corrosion current density $i_{corr,}$, and are shown in Fig. 6. At the same time, their correlation coefficient R^2 is 0.984322, indicating that the fit has a high degree of accuracy. The MAPE error determined in the testing process was observed to be 0.000035.

It can be seen from Figs. 5 and 6 that most of the points lie on or very close to the centre line, and this reflects that the

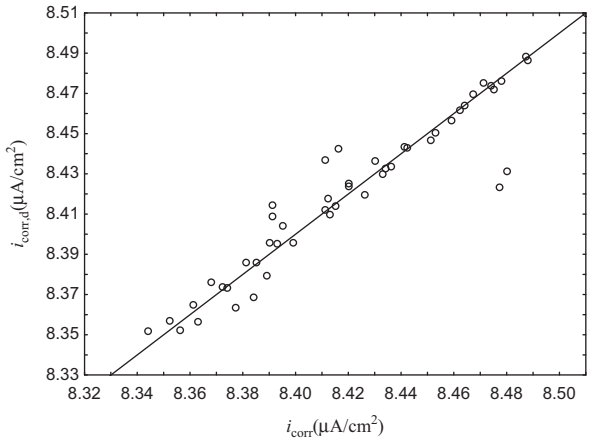

Fig. 5 – Correlation between the predicted corrosion current density and the experimentally measured corrosion current density for training (slab A).

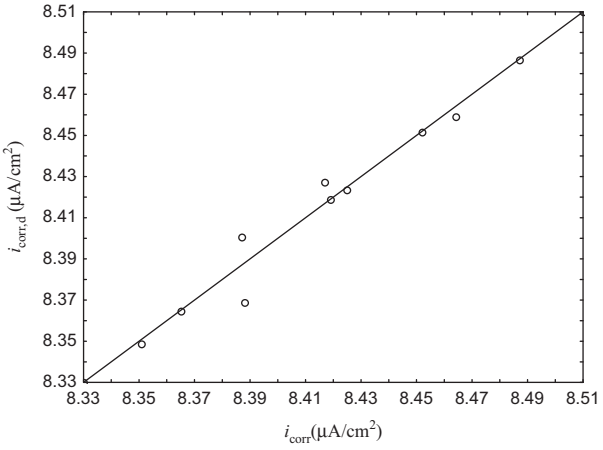

Fig. 6 – Correlation between the predicted corrosion current density and the experimentally measured corrosion current density for testing (slab A).

network output for the test data fit very well with the experimental values. It also illustrates that the MLP-NN models possess good interpolation ability.

3.2. *Slab B*

The data were also selected randomly for training and testing for slab B. A total of 70% among the data were used for training, while the remaining 15% were used for testing. The 15% of the total data were randomly selected for the MLP-NN verification process. Different numbers of neurons, between 3 and 9 in the hidden layer, were evaluated, and the resulting MAPE errors were determined. The MAPE error determined for the different number of neurons was evaluated, and in this case it was observed that when the number of neurons equals 3, the error is the lowest (Table 4). This table also lists the correlation coefficients R^2 of the applied MLP networks, and their correlation coefficients are also the highest when the number of neurons in the hidden layer is 3.

The architecture of the MLP-NN obtained for slab B is illustrated in Fig. 7. The network was generalised with an

Table 4 – Evaluation on the prediction results (slab B).

No.	MLP-NN architecture	R^2 (–)		MAPE (–)	
		Training	Testing	Training	Testing
1	**4-3-1**	**0.910938**	**0.980172**	**0.000077**	**0.000021**
2	4-4-1	0.882848	0.967200	0.000100	0.000038
3	4-5-1	0.863726	0.965994	0.000114	0.000039
4	4-6-1	0.878786	0.960291	0.000103	0.000044
5	4-7-1	0.846616	0.948758	0.000128	0.000059
6	4-8-1	0.852430	0.965025	0.000125	0.000043
7	4-9-1	0.850701	0.964157	0.000125	0.000043

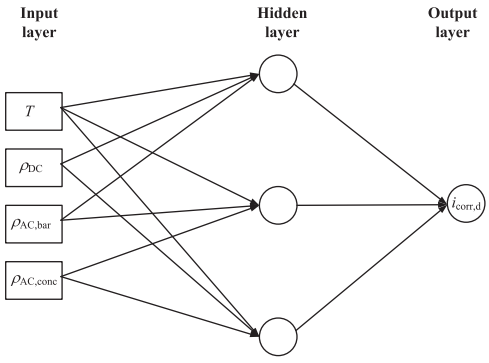

Fig. 7 – The architecture of MLP-NN obtained for slab B.

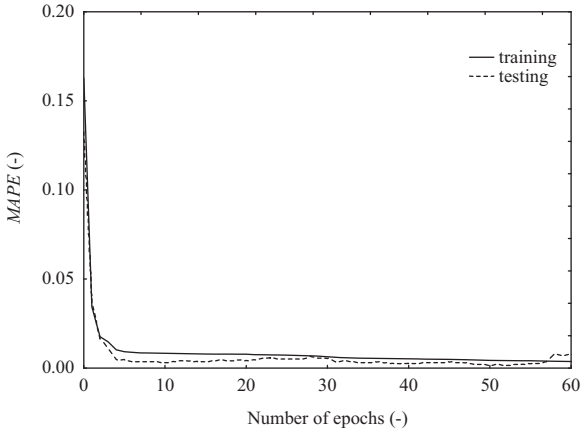

Fig. 8 – MLP-NN training and testing MAPE versus the number of epochs (slab B).

input layer, one hidden layer with 3 neurons in number and an output layer.

In this case the *MAPE* error in the training and testing process decreases rapidly with the growing number of epochs, and stabilises at a level of about 0.000090. It has been presented in Fig. 8.

The predicted values of corrosion current density $i_{corr,d}$ in the training test, estimated by the MLP-NN versus experimental values for the current density i_{corr}, are plotted in Fig. 9. The correlation coefficient is observed to be 0.910938, indicating that the fit has a very high degree of accuracy. However, the right-most point, with an estimated value 0.429 μA/cm^2 in Fig. 9, is a deviation from the centre line. This point came from the test sample numbered as 48; its

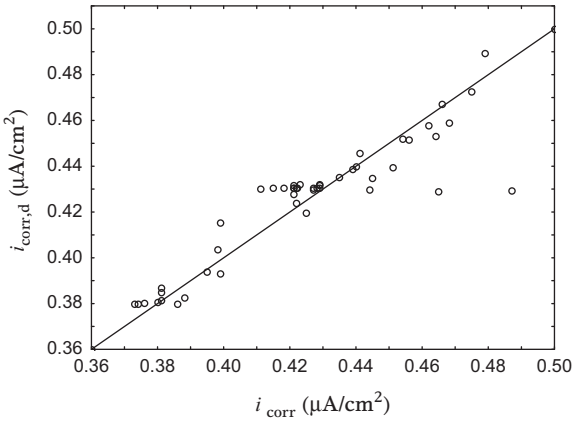

Fig. 9 – Correlation between the predicted corrosion current density and the experimentally measured corrosion current density for training (slab B).

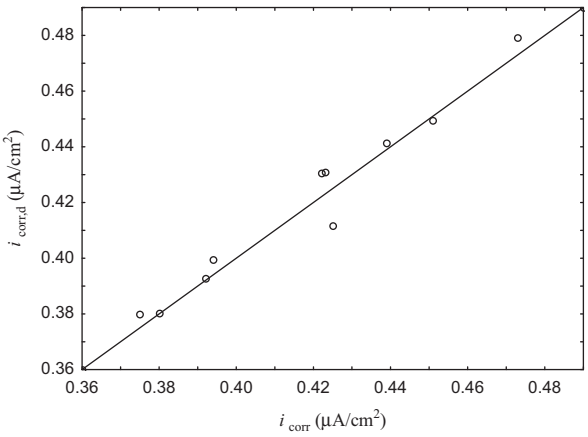

Fig. 10 – Correlation between the predicted corrosion current density and the experimentally measured corrosion current density for testing (slab B).

target value (0.487 μA/cm^2) is the largest among all of the 48 training samples. It is proper to note that the *MAPE* error in this case was observed to be 0.000077.

The predicted values of corrosion current density $i_{corr,d}$ in the testing investigation estimated by the MLP-NN versus the experimental values for the current density i_{corr} are shown in Fig. 10. The results clearly show that their correlation coefficient is, at the same time, 0.980172, thus indicating that the fit has a very high degree of precision. The *MAPE* error

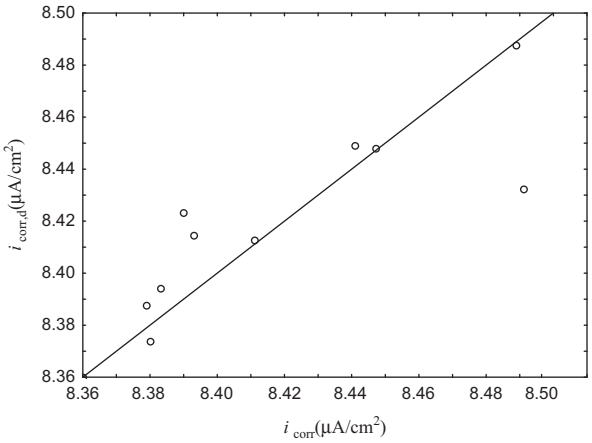

Fig. 11 – Correlation between the predicted corrosion current density and the experimentally measured corrosion current density for MLP-NN verification (slab A).

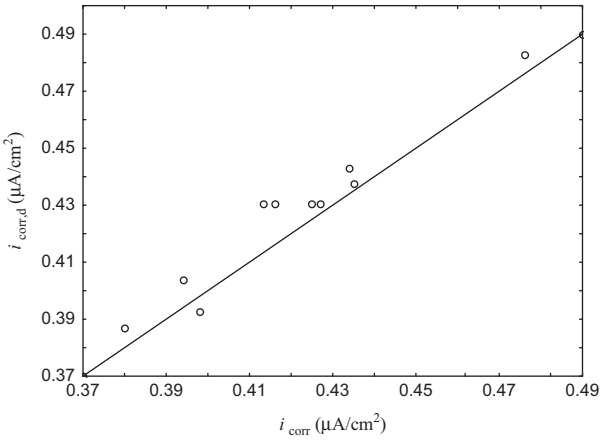

Fig. 12 – Correlation between the predicted corrosion current density and the experimentally measured corrosion current density for MLP-NN verification (slab B).

determined in the testing investigation was observed to be 0.000021.

It can be seen from Figs. 9 and 10 that most points lie on or very close to the straight line corresponding to the ideal mapping, which reflects that most of the predicted values are in good agreement with the experimental values. It also illustrates that the MLP-NN models possess good interpolation ability.

3.3. *MLP-NN verification*

In this section experimental verification of the neural network is described. The results of training and testing for slab A and slab B show that the MLP-NN correctly maps the training data and correctly identifies the testing data. However, to check ANN model generalisation capability, the data were divided into sets of 15% of the total data MLP-NN verification records for slab A and slab B.

In the MLP-NN verification process for slab *A*, the predicted values of corrosion current density $i_{corr,d}$ for different times of measurement plotted against the experimentally measured values of corrosion current density i_{corr}, are presented in Fig. 11. The correlation coefficient R^2 was observed to be 0.846335, thus indicating that the fit has a very high degree of accuracy. The *MAPE* error is observed to be 0.000266.

Conversely, in the MLP-NN verification process for slab *B*, the predicted values of corrosion current density $i_{corr,d}$ for different times of measurement plotted against the experimentally measured values of corrosion current density i_{corr}, are shown in Fig. 12. The correlation coefficient was observed to be 0.982395, thus indicating that the fit has a very high degree of accuracy. The results clearly show that the *MAPE* error determined in the MLP-NN verification process was observed to be 0.000027.

4. Conclusions

In this paper the model for steel corrosion current density under four different parameters was set up by using the MLP-NN approach.

The significance of the work results illustrates that the predicted *MAPE* errors of the MLP-NN models are small for the two sets of training and testing data. At the end of this study, model generalisation capability was verified separately for slab A and slab B. The research presented indicates that it is possible to predict the corrosion current density by artificial neural networks, particularly by the MLP-NN, and on the basis of parameters determined by two non-destructive resistivity measurement techniques.

These indicate that the MLP-NN model has a theoretical value in the prediction of the corrosion current rate of steel in concrete using corrosion current density without the need for a connection to the steel reinforcement. Thus, the model based on MLP-NN has a potential practical significance and can be further enhanced by increasing the number of training samples, a wider range of the concrete's resistivity, corrosion current density or concrete humidity.

REFERENCES

[1] X. Shia, N. Xiec, K. Fortunea, J. Gongd, Durability of steel reinforced concrete in chloride environments: an overview, Construction and Building Materials 30 (2012) 125–138.
[2] T. Blaszczynski, The influence of crude oil products on RC structure destruction, Journal of Civil Engineering and Management 17 (1) (2011) 146–156.
[3] R. Melchers, Modelling immersion corrosion of structural steels in natural fresh and brackish waters, Corrosion Science 48 (2006) 4174–4201.
[4] J. Liu, Y. Lin, X. Li, Numerical simulation for carbon steel flow-induced corrosion in high-velocity flow seawater, Anti-Corrosion Methods and Materials 55 (2008) 66–72.
[5] M. Hajeeh, Estimating corrosion: a statistical approach, Materials & Design 24 (2003) 509–518.
[6] C. Andrade, C. Alonso, Test methods for on-site corrosion rate measurement of steel reinforcement in concrete by means of the polarization resistance method, Materials and Structures 37 (2004) 623–643.
[7] S. Millard, Measuring the corrosion rate of reinforced concrete using linear polarization resistance, Concrete (2003) 36–38.
[8] M. Grantham, M. Associates, H. Barnet, J. Broomfield, The use of linear polarisation corrosion rate measurements in aiding

rehabilitation options for the deck slabs of a reinforced concrete underground car park, Construction and Building Materials 11-4 (1997) 215–224.
[9] D. Law, S. Millard, J. Bungey, Linear polarisation resistance measurements using a potentiostatically controlled guard ring, NDT&E International 1 (2000) 15–21.
[10] F. Wenner, A method of measuring earth resistivity, Bulletin of the Bureau of Standards 12 (1912) 469–478.
[11] U. Angst, B. Elsener, C. Larsen, O. Vennesland, Chloride induced reinforcement corrosion: rate limiting step of early pitting corrosion, Electrochimica Acta 56 (2011) 5877–5889.
[12] B. Hope, A. Ip, D. Manning, Corrosion and electrical impedance in concrete, Cement and Concrete Research 15-3 (1985) 525–534.
[13] J. Gulikers, Theoretical considerations on the supposed linear relationship between concrete resistivity and corrosion rate of steel reinforcement, Materials and Corrosion 56 (5) (2005) 393–403.
[14] W. Morris, A. Vico, M. Vazquez, S. de Sanchez, Corrosion of reinforcing steel evaluated by means of concrete resistivity measurements, Corrosion Science 44 (1) (2002) 81–99.
[15] A. Ramezanianpour, A. Pilvar, M. Mahdikhani, F. Moodi, Practical evaluation of relationship between concrete resistivity, water penetration, rapid chloride penetration and compressive strength, Construction and Building Materials 25 (5) (2011) 2472–2479.
[16] W. McCarter, G. Starrs, S. Kandasami, R. Jones, M. Chrisp, Electrode configurations for resistivity measurements on concrete, ACI Materials Journal 106 (3) (2009) 258–264.
[17] A. Schuetze, W. Lewis, C. Brown, W. Geerts, A laboratory on the four-point probe technique, American Journal of Physics 72 (2) (2004) 149.
[18] L. Sadowski, New non-destructive method for linear polarisation resistance corrosion rate measurement, Archives of Civil and Mechanical Engineering 10 (2) (2010) 109–116.
[19] J. Hola, M. Ksiazek, Research on usability of sulphur polymer composite for corrosion protection of reinforcing steel in concrete, Archives of Civil and Mechanical Engineering 9 (1) (2009) 47–59.
[20] M. Ksiazek, The experimental and innovative research on usability of sulphur polymer composite for corrosion protection of reinforcing steel and concrete, Composites. Part B: Engineering 42 (5) (2011) 1084–1096.
[21] T. Blaszczynski, Assessment of RC structures influenced by crude oil products, Archives of Civil and Mechanical Engineering 11 (1) (2011) 5–17.
[22] S. Haykin, Neural Networks: A Comprehensive Foundation, Prentice Hall, 1999.
[23] J. Hola, K. Schabowicz, New technique of nondestructive assessment of concrete strength using artificial intelligence, NDT&E International 38 (2005) 251–259.
[24] N. Langaros, M. Papadrakakis, Neural network based prediction schemes of the non-linear seismic response of 3D buildings, Advances in Engineering Software 44 (2012) 92–115.
[25] A. Kaveh, M. Ahangaran, Discrete cost optimization of composite floor system using social harmony search model, Applied Soft Computing 12 (2012) 372–381.
[26] B. Hola, K. Schabowicz, Estimation of earthworks execution time cost by means of artificial neural networks, Automation in Construction 19 (2010) 570–579.
[27] V. Kappatos, A.N. Chamos, S.G. Pantelakis, Assessment of the effect of existing corrosion on the tensile behaviour of magnesium alloy AZ31 using neural networks, Materials & Design 31 (2010) 336–342.
[28] M. Shaw, S. Millard, T. Molyneaux, M. Taylor, J. Bungey, Location of steel reinforcement in concrete using ground penetrating radar and neural networks, NDT&E International 38 (3) (2005) 203–212.
[29] T. Parthiban, R. Ravi, G.T. Parthiban, S. Srinivasan, K.R. Ramakrishnan, M. Raghavan, Neural network analysis for corrosion of steel in concrete, Corrosion Science 47 (2005) 1625–1642.
[30] S. He, Y. Zou, D. Quan, H. Wang, Application of RBF neural network and ANFIS on the prediction of corrosion rate of pipeline steel in soil, Recent Advances in Computer Science and Information Engineering, Lecture Notes in Electrical Engineering 124 (2012) 639–644.
[31] I. Topçu, A. Boğa, F. Hocaoğlu, Modelling corrosion currents of reinforced concrete using ANN, Automation in Construction 18 (2009) 145–152.
[32] Y. Wen, C. Cai, X. Liu, J. Pei, X. Zhu, T. Xiao, Corrosion rate prediction of 3C steel under different seawater environment by using support vector regression, Corrosion Science 51 (2009) 349–355.
[33] R. Eberhart, Computational intelligence PC tools, in: Proceedings of AP Professional, New York, 1996.
[34] K. Halawa, A method to improve the performance of multilayer perceptron by utilizing various activation functions in the last hidden layer and the least squares method, Neural Processing Letters 34 (3) (2011) 293–303.
[35] G. Panchal, A. Ganatra, P. Kosta, D. Panchal, Behaviour analysis of multilayer perceptrons with multiple hidden neurons and hidden layers, International Journal of Computer Theory and Engineering 3 (2) (2011) 332–337.
[36] W. Dawson, R. Wilby, An artificial neural network approach to Rainfall–Runoff modelling, Hydrological Sciences Journal 43 (1) (1998) 47–66.
[37] M. Stigler, Francis Galton's account of the invention of correlation, Statistical Science 4 (2) (1989) 73–79.
[38] S. Smith, T. Sincich, Stability over time in the distribution of population forecast errors, Demography 25 (1988) 461–474.
[39] D. Rumelhart, G. Hinton, R. Williams, Learning representations by back-propagating errors, Nature 323 (1986) 533–536.
[40] W. Chien, L. Chen, C. Wei, H. Hsu, T. Wang, Modeling slump flow of high-performance concrete using back-propagation network, Applied Mechanics and Materials 20 (23) (2010) 838–842.
[41] H. Moon, J. Kim, Intelligent crack detecting algorithm on the concrete crack image using neural network, in: Proceedings of the 28th ISARC, Seoul, Korea, 2011, pp. 1461-–1467.
[42] B. Taylor, M. Darrah, C. Moats, Verification and validation of neural networks: a sampling of research in progress, in: Kevin L. Priddy, Peter J. Angeline (Eds.), Intelligent Computing: Theory and Applications, Proceedings of SPIE 5103 (2003) 8–16.